



# Planar band-notched ultra-wideband antenna with square-looped and end-coupled resonator

S.-J. Wu J.-H. Tarng

Department Communication Engineering, National Chiao Tung University, Hsinchu City, Taiwan  
 E-mail: [sungjungwu.cm96g@nctu.edu.tw](mailto:sungjungwu.cm96g@nctu.edu.tw)

**Abstract:** A square-looped and an end-coupled resonator used in a planar ultra-wideband (UWB) antenna to achieve band-notched performance are presented here. To obtain notched performance in the wireless local area network band, both the square-looped and end-coupled resonator are designed and placed in a fork-shaped UWB antenna centre. The characteristics and schematic equivalent circuit of each resonator are also discussed. Parametric studies of a fork-shaped antenna with square-looped resonator are given as an example to explore the operating mechanism. Accordingly, the band-notched antenna can effectively select target bands by adjusting different resonator structures. The proposed antenna features flat gain-frequency response and group delay as well as 10–25 dB gain suppression in the notched band.

## 1 Introduction

Since the Federal Communication Commission (FCC) allowed the use of the 3.1–10.6 GHz unlicensed band and an EIRP less than  $-41.3$  dBm/MHz for ultra-wideband (UWB) communication, UWB technology has been widely investigated for short-range wireless applications. Compared with narrow band systems, UWB technology has better system performance such as high-resolution radar imaging, rejection of multipath cancellation effects and transmission of high data-rate signals because of its extremely wide bandwidth [1–3].

UWB antennas have to operate across a very wide bandwidth with consistent polarisation, radiation patterns, gain response and group delay. A number of technologies have been proposed for wide-band impedance matching. Initially, the travelling wave concept was extensively applied in the slot and bowtie-type antennas in order to utilise the wide bandwidth and omni-radiation patterns [4–6]. However, these antennas usually have inherently larger size and need a larger ground plane. To overcome this problem, many researchers have proposed the aperture antenna. The advantages of aperture antennas are bandwidth enhancement and ease of integration with RF circuits for low-cost manufacturing processes [7, 8]. In aperture antenna schemes, the antenna usually consists of a widened slot/aperture and an exciting stub. The bandwidth of aperture antennas, especially for low frequencies, is determined by the size of the exciting stub and the distance between the exciting stub and the edge of the aperture. Finally, many monopole antennas with flat/taper structure are proposed for bandwidth enhancement. These antennas with various shapes, such as circular, triangular and elliptic, achieve broad bandwidth operation and compact antenna size for UWB applications [9–12].

Existing wireless local area network (WLAN), such as IEEE 802.11a or HiperLAN/2, may interfere with UWB operation. Therefore UWB systems use extra band-stop filters to suppress unwanted signals in some applications. Nevertheless, the use of filters increases the complexity and the cost of UWB systems. Several studies propose UWB antennas with filtering properties in the WLAN band for removing the additional requirement of a band-stop filter in the system [13–20]. Thus, UWB antennas not only require wide impedance matching, stable radiation characteristics, compact size and low manufacturing cost but also provide a notched band to minimise potential interferences.

The band-notched technique is important in UWB antenna designs and can be categorised according to three methods. One is to cut a thin slit in the antenna structure [14–16]. Another technique is to add a plastic strip in the aperture area of the antenna or a nearby radiator that forms a resonant structure and leads to a sudden change in the impedance in the notched band [17, 18]. In above two methods, the notched frequency is mainly determined by the length of slit/strip. Generally, the length of slit/strip is usually proportional to (i) half a wavelength of the notched frequency for both the short-end slit and open-end strip and (ii) a quarter of a wavelength of the notched frequency for open-end slit. The other type is to directly add the narrow-band resonator in the antenna structure [19–24]. In contrast to the two above-mentioned methods, the notched frequency and bandwidth of the antenna depend mostly on the resonant frequency and quality factor of the resonator, respectively.

In this paper, two kinds of proposed resonators, a square-looped resonator and an end-coupled resonator, are used, respectively, in a fork-shaped UWB antenna to achieve the gain suppression in the notched band. The square-looped resonator consists of two square loops whose physical

length approximates half a wavelength at the notched frequency. Meanwhile, the end-coupled resonator is composed of a strip line with a pair of quarter wavelength folded open stubs. Compared with the band-notched methods using thin slits and plastic strips, the proposed resonators have several advantages.

1. The resonator is placed in the centre of the fork-shaped antenna and does not add to the size of the antenna.
2. The resonator interferes only slightly with the fork-shaped antenna's performance except within the notched band.
3. The resonator has a simple geometry with fewer parameters, which releases computation load in the optimisation process.
4. The resonator demonstrates good notched band performance such as narrow notched bandwidth, fast roll-off rate as well as 10–25 dB gain suppression (generally, the measured gain suppression of thin slits and plastic strips are usually less than 10 dB [14–17]).

Compact sized antennas ( $35 \times 20 \text{ mm}^2$ ) have been successfully designed, built and verified. The proposed antennas have promising characteristics in terms of impedance matching, radiation patterns, gain response and group delay over the entire UWB band. Meanwhile, the proposed antennas show good notched performance such as a fast roll-off rate, good gain suppression ability and narrow notched bandwidth at the notched band. In Section 2, a fork-shaped UWB antenna with a square-looped resonator and end-coupled resonator is presented. The geometry and design concept of each resonator is discussed. The comparison between the square-looped resonator and the tapped-line coupled resonator in [22] is further discussed. In Section 3, a parametric study of the proposed antenna with the square-looped resonator is used to explain the basic resonant behaviour. Consequently, the gain-frequency transfer function and group delay are presented. Finally, conclusions are presented in Section 4.

## 2 Antenna geometry and design concept

### 2.1 Geometry of the proposed antenna

Fig. 1 shows the geometry of the proposed antenna, which consists of a fork-shaped UWB antenna and a square-looped resonator. The fork-shaped UWB antenna design is based on the triangular-shaped radiator and the U-shaped radiator in [13, 14]. The bevel profile of the fork-shaped UWB antenna enhances the wide operating bandwidth, especially for higher frequencies because it reduces the impedance variation from the microstrip line to free space. Meanwhile, the lowest frequency is determined by the length of  $L_1 + L_2 + W_2$ . Furthermore, the majority of the electric currents are concentrated around the narrow portion of the fork-shaped UWB antenna. Hence, the resonator position inside the antenna not only determines the band-notched characteristics, but also nearly retains the original essential characteristics of the antenna. The inner cutting triangular area ( $0.5 \times 2.5 \text{ mm} \times 14 \text{ mm}$ ) is applied here to place the proposed resonators. Ansoft HFSS 9.2 is used for simulations, whereas an Agilent E8362B performance network analyser is used for the measurements. The antenna was fabricated on a  $35 \text{ mm} \times 30 \text{ mm} \times 0.77 \text{ mm}$  Rogers RO4003 substrate with dielectric constant  $\epsilon_r = 3.28$  and loss tangent = 0.004 at 10 GHz. The final design parameters are  $W_1 = 14$ ,  $W_2 = 8.3$ ,  $W_3 = 2$ ,  $W_4 = 1.4$ ,

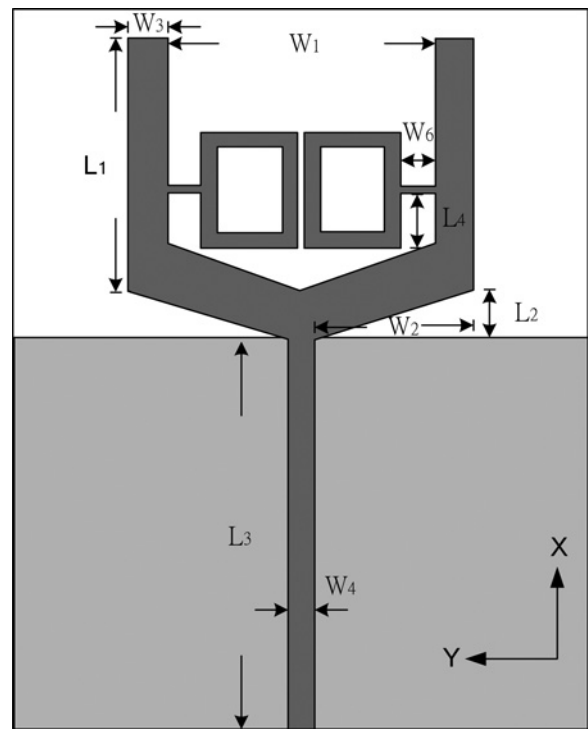


Fig. 1 Geometry of proposed antenna

$W_5 = 1.8$ ,  $W_6 = 0.8$ ,  $W_7 = 5$ ,  $L_1 = 13$ ,  $L_2 = 2.5$ ,  $L_3 = 20$ ,  $L_4 = 2.5$ ,  $L_5 = 0.4$ ,  $L_6 = 2.8$ ,  $L_7 = 2.8$ ,  $L_8 = 6$ ,  $g = 0.4$ , where the measurement units are in mm.

Fig. 2 shows the simulated and measured voltage standing wave ratio (VSWR). The measured result agrees with the simulated one. It demonstrates the resonant behaviour, which leads to the desired impedance mismatching near the notched frequency at 5.6 GHz. The notched band reveals the narrow bandwidth and the fast roll-off rate because of the high-quality factor and the appropriate position of the resonator.

### 2.2 Square-looped resonator and end-coupled resonator

Figs. 3a and b show the square-looped resonator and tapped-line coupled resonator of [22], respectively. The short strip,  $W_5$ , connects the proposed resonator and the fork-shaped UWB antenna. Basically, Figs. 3a and b have a similar

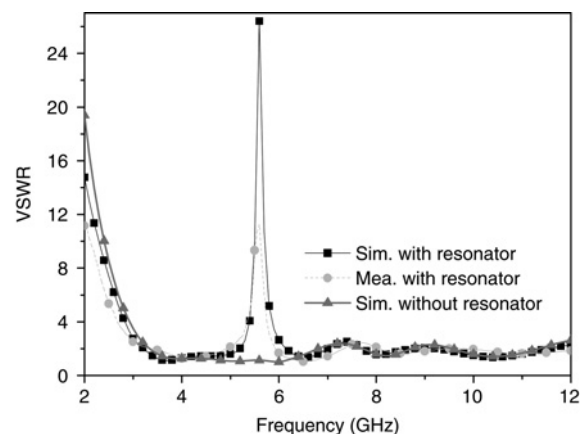
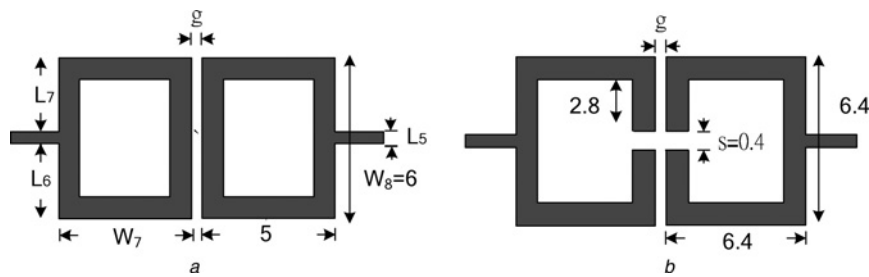


Fig. 2 Measured and simulated VSWR of fork-shaped UWB antenna with square-looped resonator



**Fig. 3** Geometries of square-looped resonator and tapped-line coupled resonator

a Square-looped resonator structure  
b Tapped-line coupled resonator of [22]

geometry. The difference between them is the gap of  $s$ . Hence, the structure in Fig. 3a can be treated as a half-wavelength ring resonator, whereas the structure in Fig. 3b is an open-ended resonator that consists of a pair of quarter wavelength strips. There are two points worth noting when the fork-shaped UWB antenna uses the resonator structure of Fig. 3b. First, the fringe field at the open-end of resonator is decreased because the resonator is floating. Second, when a resonator has differing lengths for the two strips, the antenna may have two notched frequencies.

The square-looped resonator can be represented by the lossless parallel-tuned circuit as shown in Fig. 4. The mutual coupling,  $C_m$ , is determined by the gap  $g$ . The notched frequency is mainly determined by the resonance of each sub-loop ( $L_{eq}$  and  $C_{eq}$ ) and the gap  $g$  ( $C_m$ ). Through the simulation, the gap  $g$  slightly affects the resonant frequency even if it varies from 0.2 to 1.4 mm. Thus, for notched frequency controllability, the variation of mutual coupling is not a key factor but the length is dominant.

Fig. 5 shows the simulated admittances of the proposed antenna as shown in Fig. 1 and the square-looped resonator. The resonant frequency of the square-looped resonator is quite similar to the notched frequency of the proposed

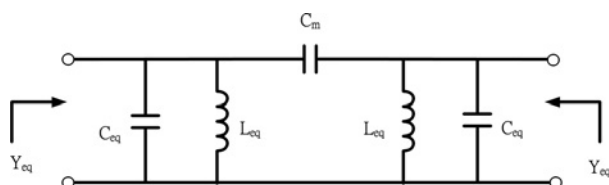


**Fig. 4** Schematic equivalent circuit of square-looped resonator

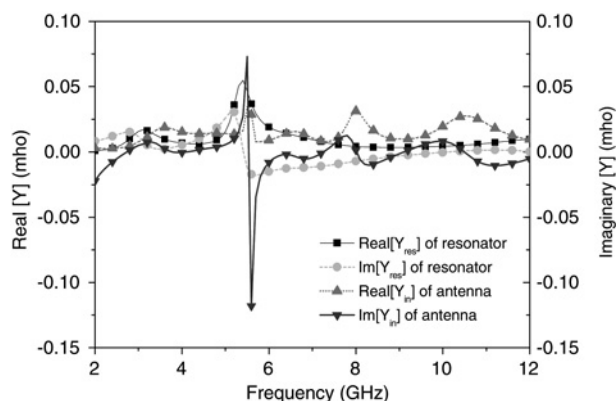


**Fig. 5** Simulated admittance of the proposed antenna with the square-looped resonator

antenna. It demonstrates parallel resonant behaviour, which leads to the desired impedance mismatching at 5.6 GHz.

Figs. 6a and b illustrate a proposed end-coupled resonator and its equivalent circuit, respectively. The end-coupled resonator has a compact size,  $4.4 \times 4.4 \text{ mm}^2$ , and is composed of a strip line with a pair of folded open stubs that form the coupled loads,  $C_{m2}$ , as shown in Fig. 6b. In this case, the resonant frequency of the resonator is determined by the length of the folded open stubs and coupled loads.

Fig. 7 shows the simulated and measured VSWR of the fork-shaped UWB antenna with the end-coupled resonator. The parameters of the end-coupled resonator are as follows:  $W_8 = 4.4$ ,  $W_9 = 0.8$ ,  $W_{10} = 5.8$ ,  $L_9 = 4.4$ ,  $L_{10} = 0.4$ ,  $L_{11} = 1.0$  and  $S = 0.4$ , where the measurement units are in mm. As shown in Fig. 4, the measured result agrees with the simulated one. The impedance of the end-coupled resonator is quite similar to that of the square-looped resonator and is not shown here for brevity.

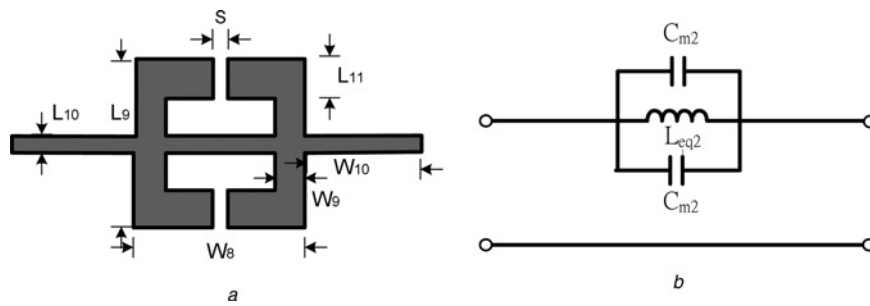
### 3 Performance of fork-shaped UWB antenna with square-looped resonator

Because the performance of both the square-looped resonator and end-coupled resonator are similar, the square-looped resonator is discussed below for the sake of brevity. Hence, in the following subsections, the geometric parameters of the square-looped resonator based on its length, feeding position and position are investigated. The measured patterns and gain response against frequency at eight angles as well as group delay are presented below.

#### 3.1 Parametric study

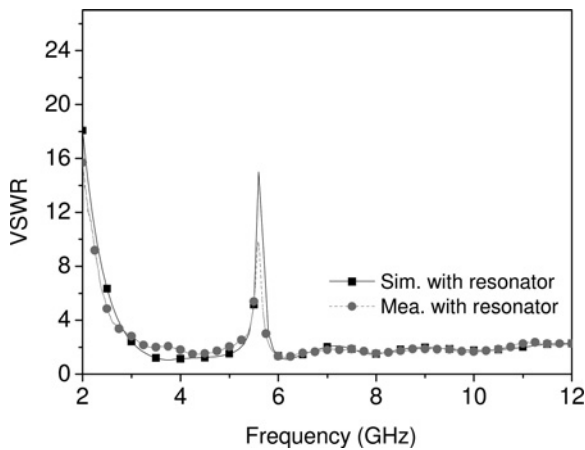
Fig. 8 depicts the VSWR for various lengths of the square-looped resonator. It is clearly seen that the length of the square-looped resonator has a significant effect on the notched frequency. The notched frequency shifts from around 5.2 GHz to 6.3 GHz as the length of the square loop changes from 20 to 24 mm. ( $L_8$  changes from 5 to 7 mm). This is because of the fact that the resonant frequency of the square-looped resonator is inversely proportional to the length of the resonator.

Fig. 9 shows the VSWR against the various input positions of the square-looped resonator. In this case, only the strip,  $W_5$ , moves in the  $x$ -direction. The location of the short strip in the  $x$ -orientation has a significant effect on the notched frequency. Compared with the resonant frequency variation of both the resonator and proposed antenna in the same condition, the variation of the proposed antenna is



**Fig. 6** Proposed end-coupled resonator and its equivalent circuit

- a End-coupled resonator structure
- b Schematic equivalent circuit of end-coupled resonator



**Fig. 7** Measured and simulated VSWR of the fork-shaped UWB antenna with end-coupled resonator

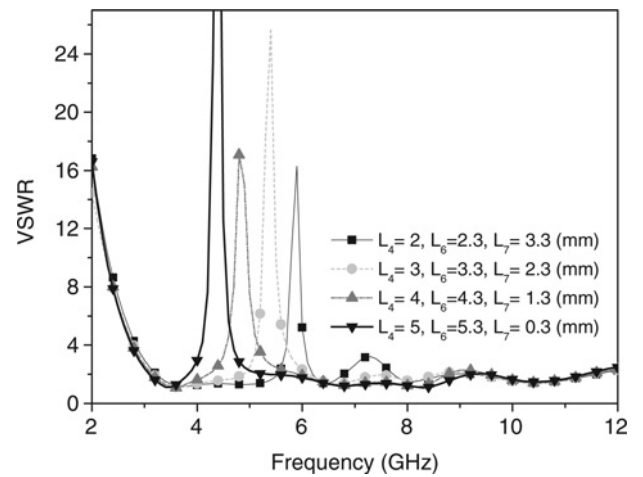


**Fig. 9** VSWR against the various input positions of the square-looped resonator

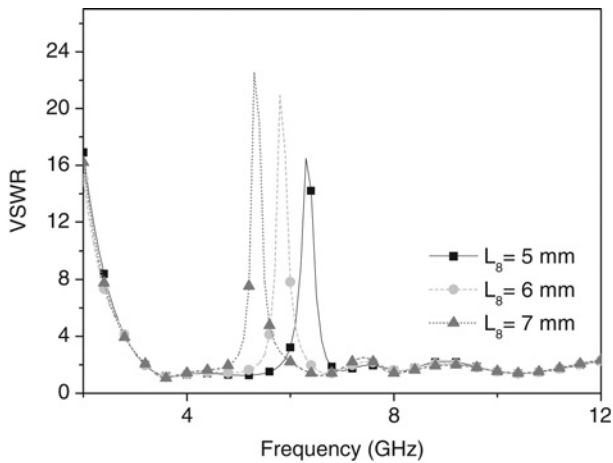


**Fig. 8** VSWR for various lengths of the square-looped resonator

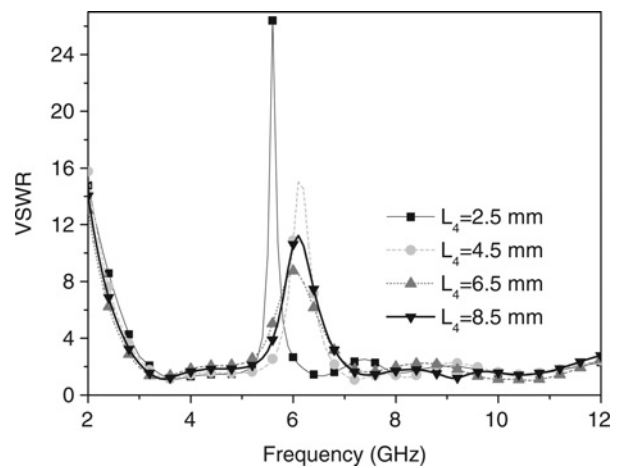


**Fig. 10** VSWR against the various positions of the resonator in the x-orientation

significantly larger than that of the resonator. It is implied that the part of the fork-shaped UWB antenna from the microstrip line to the input position of resonator affects the notched frequency because extra inductance is added to the resonator. When a resonator is treated as part of the radiator, the path from the signal source to the resonator can be modelled as an extra circuit network, which affects the notched frequency and external quality factor of the whole antenna in the notched band.

Fig. 10 shows the VSWR against the various positions of the resonator in the *x*-orientation, that is, various values of  $L_4$  while the resonator structure is fixed. When the resonator is placed at the near end of the fork-shaped UWB antenna, the mid frequency of the notched band slightly changes, while the bandwidth of the notched band is significantly larger. This implies that when the resonator is placed near the end of the fork-shaped antenna; the external quality

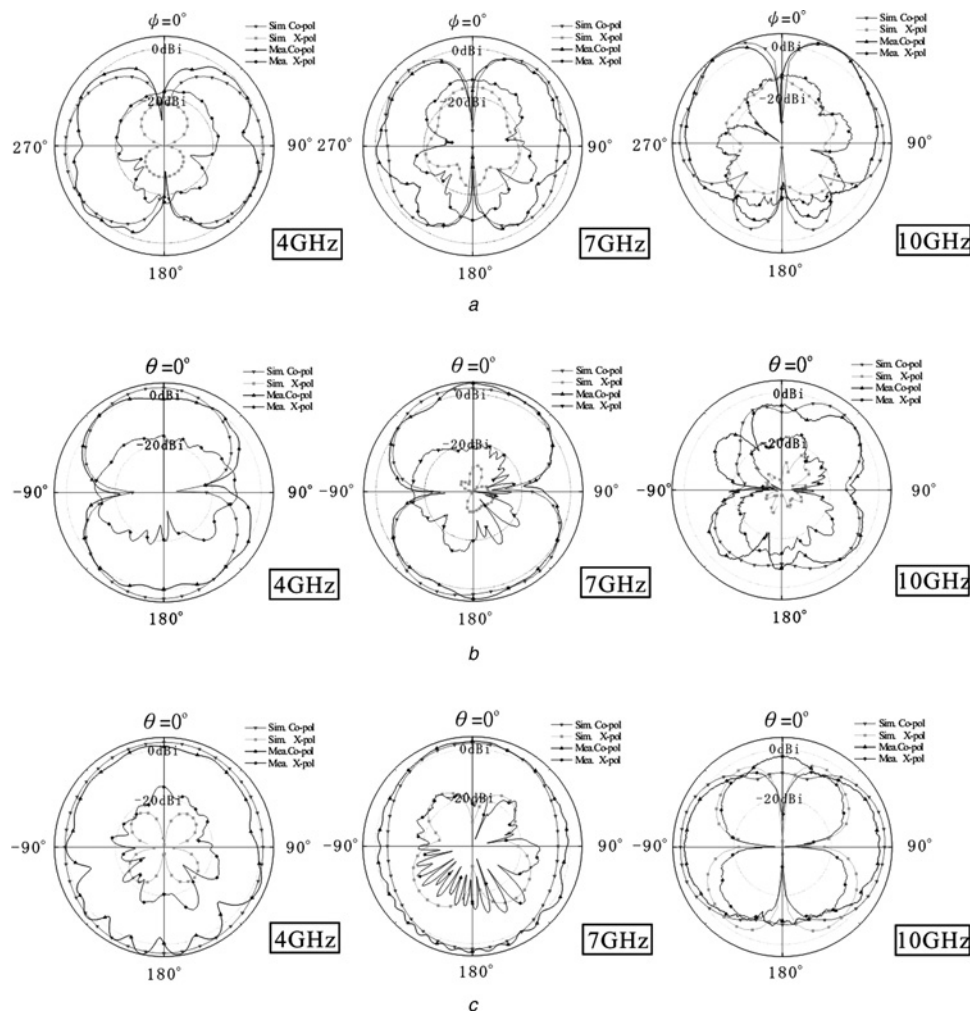


**Fig. 11** Measured and simulated radiation patterns at

- a  $xy$ -plane  
 b  $xz$ -plane  
 c  $yz$ -plane (unit, dBi)

factor reduces and the bandwidth of the notched band increases simultaneously.

### 3.2 Radiation patterns, gain response and group delay

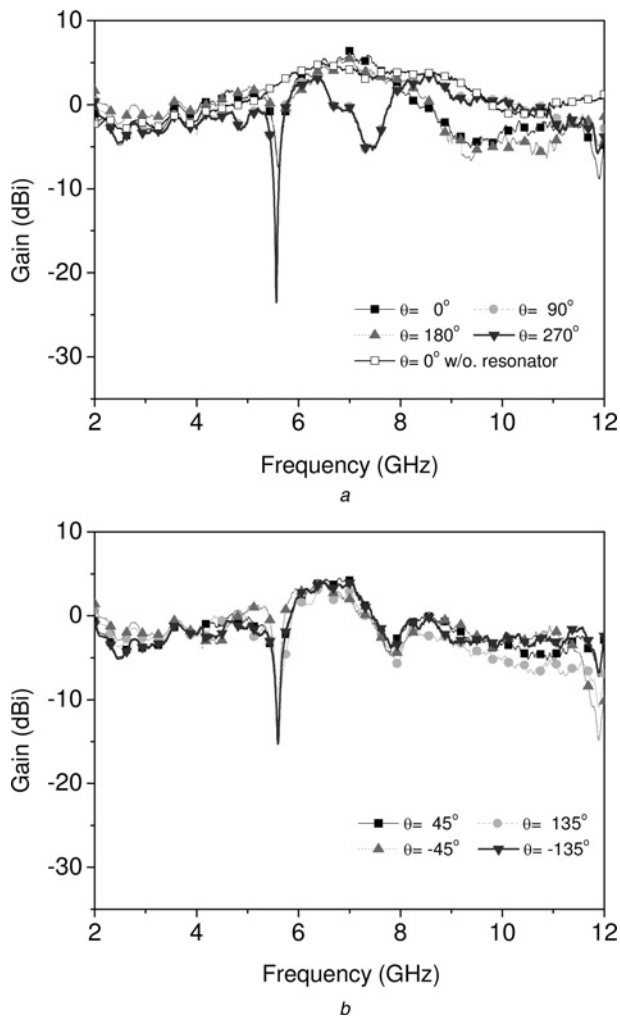
The antenna radiation patterns, gain response and group delay were measured in a  $7.0 \times 3.6 \times 3.0 \text{ m}^3$  anechoic chamber with an Agilent E8362B network analyser along with NSI2000 far-field measurement software.

Fig. 11 shows the measured and simulated radiation patterns in the  $xy$ -,  $xz$ - and  $yz$ -planes at 4, 7 and 10 GHz, respectively. The measured patterns agree with the simulated ones. Referring to Figs. 11a and b, the co-polarisation patterns are roughly dumbbell-like shapes and the cross-polarisation levels are much lower than the co-polarisation levels. In Fig. 11c, the co-polarisation patterns have omni-directional shapes at lower frequencies and dumbbell-like shapes at higher frequencies. The cross-polarisation level rises considerably as frequency increases because the resonator directly integrated into antenna layout produces a substantial level of  $y$ -oriented radiation. The discrepancies in cross-polarisations can be attributed to the

interference of the coaxial cable and the absorbers used in the measurement arrangement.

In measuring the antenna gain frequency response, an EMCO 3115 double-ridge horn antenna with a constant group delay of 680 ps is used as a reference antenna for calibration. Fig. 12 illustrates the measured gain frequency responses in the  $yz$ -plane at eight angles, ranging from  $-180^\circ$  to  $180^\circ$  with  $45^\circ$  intervals. According to Fig. 12, the range of gain suppression is from 10 to 25 dB for these eight angles at the target notched band. The notched frequencies are quite similar at the observation angles. The notched bandwidth is significantly narrower because of the fast roll-off rate and high-quality factor of the proposed resonator.

Fig. 13 presents the measured group delay of the proposed antenna. Except for the notched band, the variation of group delay variation over the 3.1–10.6 GHz is less than 860 ps with an average of 1.6 ns as the spatial angle varies. In the notched band, the impedance mismatch between the proposed antenna and far-field measurement system causes inaccurate and negative group delay. Figs. 12 and 13 show that the proposed antenna have good time/frequency characteristics and a small pulse distortion over the UWB-operated band.



**Fig. 12** Measured gain response

a  $\theta = 0^\circ, \theta = 90^\circ, \theta = 180^\circ, \theta = 270^\circ$

b  $\theta = 45^\circ, \theta = 135^\circ, \theta = -45^\circ, \theta = -135^\circ$

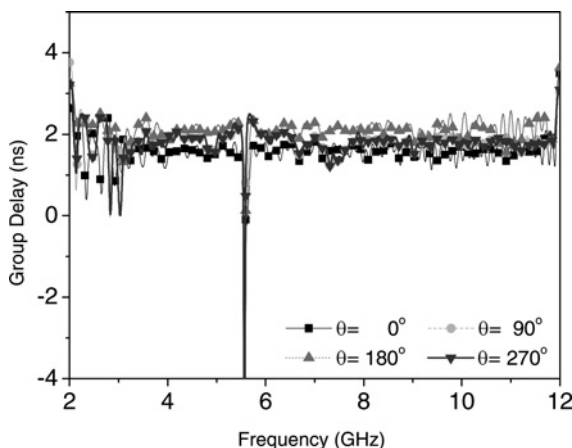


**Fig. 13** Measured group delays

## 4 Conclusion

A band-notched monopole UWB antenna using a square-looped resonator and an end-coupled resonator has been presented. By using two resonators, the proposed antenna has a narrower notched bandwidth and good gain

suppression ability in the WLAN band. The set of parameter studies of the proposed antenna provides brief guidelines for the band-notched antenna design. Evaluations of return loss, radiation patterns, gain responses and group delay confirm the antenna performance. These features of the proposed antenna demonstrate that the proposed antenna is suitable for UWB communicational applications and prevents interference from WLAN systems.

## 5 Acknowledgments

The authors thank the Wireless Communication and Electromagnetism Application Lab of the National Taiwan University of Science and Technology, Taiwan, R.O.C., for supporting the far-field measurements. This work was also supported by the National Science Council, R.O.C., under Grant No. NSC 98-2221-E-009-051 and Grant No. NSC 98-2219-E-009-001.

## 6 References

- Task Group 3a Homepage. Available at: <http://www.ieee802.org/15/pub/TG3a.html>
- Win, M.Z., Scholtz, R.A., Barnes, M.A.: 'Ultra-wide bandwidth signal propagation for indoor wireless communications'. IEEE Int. Conf. on Communications, ICC 97, 'Towards the Knowledge Millennium', Montreal, 8–12 June 1997, vol. 1, pp. 56–60
- Kwon, D.-H.: 'Effect of antenna gain and group delay variations on pulse-preserving capabilities of ultrawideband antennas', *IEEE Trans. Antennas Propag.*, 2006, **54**, (8), pp. 2208–2215
- Ghosh, S.: 'Band-notched modified circular ring monopole antenna for ultrawideband applications', *IEEE Antennas Wirel. Propag. Lett.*, 2010, **9**, pp. 276–279
- Ma, T.-G., Jeng, S.-K.: 'Planar miniature tapered-slot-fed annular slot antennas for ultrawide-band radios', *IEEE Trans. Antennas Propag.*, 2005, **53**, (3), pp. 1194–1202
- Gschwendtner, E., Wiesbeck, W.: 'Ultra-broadband car antennas for communications and navigation applications', *IEEE Trans. Antennas Propag.*, 2003, **51**, (8), pp. 2020–2027
- Lin, Y.-C., Hung, K.-J.: 'Compact ultrawideband rectangular aperture antenna and band-notched designs', *IEEE Trans. Antennas Propag.*, 2006, **54**, (11), pp. 3075–3081
- Shi, C., Hallbjörner, P., Rydberg, A.: 'Printed slot planar inverted cone antenna for ultrawideband applications', *IEEE Antennas Wirel. Propag. Lett.*, 2008, **7**, pp. 18–21
- Chen, Z.N., See, T.S.P., Qing, X.: 'Small printed ultrawideband antenna with reduced ground plane effect', *IEEE Trans. Antennas Propag.*, 2007, **55**, (2), pp. 383–388
- Mao, S.-G., Chen, S.-L.: 'Frequency- and time-domain characterizations of ultrawideband tapered loop antennas', *IEEE Trans. Antennas Propag.*, 2007, **55**, (12), pp. 3698–3701
- Chang, K., Kim, H., Yoon, Y.J.: 'Ultra-wideband antenna with improved gain characteristics', *IET Microw. Antennas Propag.*, 2008, **2**, (5), pp. 512–517
- Abbosh, A.M., Bialkowski, M.E.: 'Design of ultrawideband planar monopole antennas of circular and elliptical shape', *IEEE Trans. Antennas Propag.*, 2008, **56**, (1), pp. 17–23
- Chang, D.-C., Liu, M.-Y., Lin, C.-H.: 'A CPW-fed U type monopole antenna for UWB applications'. 2005 IEEE Antennas and Propagation Society Int. Symp., 3–8 July 2005, vol. 2A, pp. 512–515
- Cho, Y.J., Kim, K.H., Choi, D.H., Lee, S.S., Park, S.-O.: 'A miniature UWB planar monopole antenna with 5-GHz band-rejection filter and the time-domain characteristics', *IEEE Trans. Antennas Propag.*, 2006, **54**, (5), pp. 1453–1460
- Chawanonphithak, K., Phongcharoenpanich, C., Kosulvit, S., Krairiksh, M.: '5.8 GHz notched UWB bidirectional elliptical ring antenna excited by circular monopole with curved slot'. Asia-Pacific Microwave Conf., APMC 2007, 11–14 December 2007, pp. 1–4
- Yao, Y., Huang, B., Feng, Z.: 'A novel ultra-wideband microstrip-line fed wide-slot antenna having frequency band-notch function'. Int. Conf. on Microwave and Millimeter Wave Technology, ICMWT '07., 18–21 April 2007, pp. 1–4
- Li, C.-S., Chiu, C.-W.: 'A CPW-fed band-notched slot antenna for UWB applications'. IEEE, Antennas and Propagation Society International Symp., AP-S 2008, 5–11 July 2008, pp. 1–4

- 18 Nikolaou, S., Amadjikpe, A., Papapolymerou, J., Tentzeris, M.M.: 'Compact Ultra Wideband (UWB) elliptical monopole with potentially reconfigurable band rejection characteristic'. Asia-Pacific Microwave Conf., APMC 2007, 11–14 December 2007, pp. 1–4
- 19 Zaker, R., Ghobadi, C., Nourinia, J.: 'Novel modified UWB planar monopole antenna with variable frequency band-notch function', *IEEE Antennas Wirel. Propag. Lett.*, 2008, 7, pp. 112–114
- 20 Hong, C.-Y., Ling, C.-W., Tam, I.-Y., Chung, S.-J.: 'Design of a planar ultrawideband antenna with a new band-notch structure', *IEEE Trans. Antennas Propag.*, 2007, 55, (12), pp. 3391–3397
- 21 Wu, S.-J., Kang, C.-H., Chen, K.-H., Tarng, J.-H.: 'A notched-band UWB planar monopole antenna using the tapped-line coupled resonator'. Asia-Pacific Microwave Conf., APMC 2009, 7–10 December 2009, pp. 2486–2489
- 22 Wu, S.-J., Chen, K.-H., Kang, C.-H., Tarng, J.-H.: 'Study of an ultrawideband monopole antenna with a Band-notched open-looped resonator', *IEEE Trans. Antennas Propag.*, 2010, 58, pp. 1890–1897
- 23 Qu, S.-W., Li, J.-L., Xue, Q.: 'A band-notched ultrawideband printed monopole antenna', *IEEE Antennas Wirel. Propag. Lett.*, 2006, 5, (1), pp. 495–498
- 24 Deng, H., He, X., Yao, B., Zhou, Y.: 'Compact band-notched UWB printed square-ring monopole antenna'. Eighth Int. Symp. on Antennas, Propagation and EM Theory, ISAPE 2008, 2–5 November 2008, pp. 1–4